Deep Space One Investigations of Ion Propulsion Plasma Environment: Initial Results

J. Wang, D.E. Brinza, J.E. Polk, M.D. Henry

Jet Propulsion Laboratory, California Institute of Technology, Pasadena, CA 91109

Abstract

Deep Space One (DS1) is the first interplanetary spacecraft operated on solar electric propulsion. One of the primary investigations on DS1 is to characterize ion propulsion induced plasma interactions and their effects on spacecraft and solar wind measurements based on two plasma diagnostic packages. This paper reports the first in situ measurements of ion propulsion induced plasma environment obtained from an interplanetary spacecraft. Initial analysis of the measurements revealed interesting correlations between the induced charge-exchange plasma environment and thruster operating conditions. Sensors near thruster exit measured charge-exchange ions with a number density of $\sim 10^6\ cm^{-3}$ and a current density of $\sim 10^{-7}\ A/cm^{-2}$ under typical thruster operating conditions, a result in good agreement with pre-flight predictions based on computer particle simulations.

1. Introduction

NASA's New Millennium Deep Space One (DS1) mission marks the beginning of interplanetary missions using spacecraft operated on solar electric propulsion. The DS1 spacecraft was launched on October 24, 1998. Using a 30cm diameter Xenon ion thruster as its primary propulsion system, DS1 successfully flew by asteroid 9969 Braille on July 28, 1999, and is currently on a trajectory for possible encounters with comets Wilson-Harrington and Borrelly in 2001. By October 1999, the ion thruster has completed a total mission thrust time of more then 3000 hours.

A primary objective of New Millennium DS1 is to flight validate solar electric propulsion for interplanetary science missions, including the characterization of ion propulsion induced interactions and their effects on spacecraft payloads, subsystems, and solar wind measurements. In ion thrusters, propellant ions are accelerated electrostatically by a system of grids to form a high velocity beam (typically with an energy of about 1 KeV). Electrons are emitted from a neutralizer for neutralization of the ion beam. The propellant that remains un-ionized also flows out of the thruster exit at a thermal speed corresponding to the thruster wall temperature. Charge-exchange collisions will occur between the fast moving propellant ions and the slow moving neutrals which generate slow moving ions and fast moving neutrals. Hence, for a spacecraft operated on ion thruster there is a continued presence of a plasma plume composed by propellant ions, neutralizing electrons, unionized neutral propellant, non-propellant efflux (i.e. material eroded and sputtered from the thruster), and a low energy plasma generated within the plume mostly due to charge-exchange collisions. (A fraction of this low energy plasma may also come from the photo-ionized neutral propellant.) It has long been recognized that the ion thruster plume may lead to a variety of plasma interactions and plume contaminations, and hence both science and engineering concerns have been raised over the potential effects from ion thruster operation.

A major plasma interaction issue is the charge-exchange plasma environment. It is well known that the low energy charge-exchange ions generated within the plume can be pushed out of the plume by local electrostatic potential and backflow to interact with the spacecraft. Although charge-exchange plasma interaction has been a subject of extensive experimental and theoretical studies(for example, see *Carruth*[1981]; *Samanta Roy et al.*[1996a,b], *Wang et al.*[1996], and references therein), there have been few comprehensive in-flight investigations due to lack of flight opportunities.

Ion thrusters have never been flown on an interplanetary spacecraft. Although a few in-flight investigations have been attempted abroad earth-orbiting spacecrafts, such as the experiments conducted on the SERT II [*Kerslake et al.*, 1971] spacecraft in a polar orbit for a mercury ion thruster and on the ATS-6 [*Worlock et al.*, 1975] spacecraft in geosynchronous orbit for a cesium ion thruster, almost all existing experimental data on ion thruster plume are obtained from ground tests of ion thrusters, with the majority of the data obtained for mercury and cesium ion thrusters [*Carruth*, 1981; *Jones et al*, 1970]. Since the density difference between the plume and the ambient plasma sensitively influences the plume potential relative to the ambient, which in turn influences the dynamics of charge exchange ions, charge-exchange plasma interactions may differ significantly in different ambient plasmas [*Wang et. al.*, 1995].

As it is impossible to create in a vacuum tank a plasma environment similar to that under typical solar wind conditions, it is difficult to quantitatively predict ion propulsion induced plasma interactions for an interplanetary spacecraft based on ground test data.

The DS1 mission provides the first ever comprehensive in-flight investigations of ion propulsion induced interactions and their effects. This paper reports initial analysis of the first in situ measurements of ion propulsion induced plasma environment obtained from an interplanetary spacecraft. Section 2 describes the DS1 ion thruster and instrumentation. Sections 3 discuss the characterization of ion thruster induced plasma environment. Section 4 contains a summary and conclusions.

2. Ion Thruster and Instrumentation

NSTAR Ion Thruster

The DS1 spacecraft is illustrated in Figure 1. A detailed description of the spacecraft can be found in [*Rayman and Lehman*, 1997].

The flight ion propulsion system is developed under the NASA Solar electric propulsion Technology Application Readiness (NSTAR) program, a joint Jet Propulsion Laboratory/Glenn Research Center effort with industry participations from Hughes Electron Dynamics (HED), Moog Inc., and Spectrum Astro, Inc. The 30 cm diameter xenon NSTAR thruster, fabricated by HED, has an input power range of 600 to 2500 W. The propellant Xe^+ ions are accelerated through a molybdenum grid to form a beam with an energy of up to 1100 eV (exit beam velocity of $v_b \simeq 3.5 \times 10^6$ cm/s). and a current of up to 1.8 A. At full thrust level, the thruster produces a thrust of 92 mN and a specific impulse of about 3100s. The propellant ions form a divergent beam with a divergence half angle about 15 to 20^o due to the curvature of the thruster exit surface. The ion beam is kept quasi-neutral by electrons emitted from the neutralizer. The propellant that remains un-ionized flows out of the thruster exit in free molecular flow with a thermal speed corresponding to the thruster wall temperature of $\sim$ 500 K. The density of the neutral plume typically remains quasi-steady due to the low charge-exchange collision rate. A detailed description of the in-flight validation of the NSTAR ion thruster is discussed in [*Polk et al.*,1999].

Instrumentation

DS1 carries two science instrument packages: the Miniature Integrated Camera and Spectrometer (MICAS) and the Plasma Experiment for Planetary Exploration (PEPE), and one ion propulsion diagnosis package: the Ion propulsion Diagnostic Subsystem (IDS). Ion propulsion related investigations are based on IDS and PEPE measurements. This paper will focus on IDS measurements. Results from PEPE measurements are reported elsewhere.

The Ion Propulsion Diagnostic Subsystem, located near the ion thruster exit, is an integrated, comprehensive set of diagnostics designed to characterize ion propulsion induced environments and contaminations. IDS is developed by the NSTAR project at JPL as part of the NSTAR ion propulsion system. IDS has several components, as shown in Figure 2. The contamination is monitored by two quartz crystal microbalances and two calorimeters. Plasma measurements are made by a retarding potential analyzer (RPA), a planar Langmuir probe (LP), and a spherical Langmuir probe. Electrostatic and electromagnetic noise measurements are made by a plasma wave antenna and a search coil magnetometer. Magnetic field measurements are made by two flux gate magnetometers. The two flux gate magnetometers are provided by the Technical University of Braunschweig, and the plasma wave antenna is provided by TRW. The rest of the sensors are built at JPL.

As the focus of this paper is on the induced plasma environment, we will only analyze data obtained from the retarding potential analyzer (IDS-RPA) and the planar Langmuir probe (IDS-LP1). IDS-RPA and IDS-LP1 are co-located at about 0.5 meter from the thruster center.IDS-RPA has a voltage range of 0 to +100 Vdc and a current range of 0 to 100 μA). The opening to the RPA is 20 cm^2. IDS-LP1 has a voltage range of -12 to +12 Vdc and a current range of -0.5 to +40 mA. The current collecting area of IDS-LP1 is 50 cm^2.

3. Characterization of Ion Thruster Induced Plasma Environment

In this section, we present an initial characterization of ion propulsion induced plasma environment for DS1 based on IDS-RPA and IDS-LP1 measurements.

During the time between the initial start of the ion engine in late November, 1998 and the completion of the deterministic thrusting for the encounter with asteroid Braille in July, 1999, the ion propulsion system has operated for a total of 1791 hours at engine power levels ranging from 0.48 to 1.94 kW [*Polk et al.*, 1999]. High-quality data was collected by IDS and PEPE for a variety of engine operating conditions. In this paper, we examine measurements obtained during a DS1 activity called S-Peak. The S-Peak data set is of particular interest because thrusting during S-Peak reached one of the highest power levels in the entire DS1 mission, which is also the the highest engine power level among all the operating conditions covered by simultaneous IDS and PEPE measurements.

Ion Thruster Operation: DS1 S-Peak

The DS1 S-Peak activity occurred on Jan 22nd, 1999. S-Peak is designed to determine peak power point for

the SCARLET arrays. The S-Peak thrusting started at 21:36 PDT. The thruster operation stepped through three thrust levels, starting at a low thrust level, then stepping to a medium, and finally a high thrust level. On the flight throttle table, the three thrust levels are defined as mission levels (ML) 6, 36, and 83, respectively. Thrusting stopped at 22:17 PDT. Figure 3 shows several key thruster performance parameters obtained from flight data, including beam current and voltage, propellant efficiency, and flow rates. The values of beam current (I_b), beam ion energy (E_b), and discharge propellant efficiency (η_d) are also listed in Table 1. The specific impulse for the three thrust levels are approximately 1972s, 2935s, and 3189s for ML 6, 36, and 83 respectively [*Polk et al.*, 1999]. The engine input power ranges from 0.47 kW at ML 6 to 1.82 kW at ML 83. ML 83 is one of the highest power levels at which the thruster has operated during the entire DS1 mission and produces the highest specific impulse among all the throttle level. Due to the short S-Peak time, the propellant flow has not reached an equilibrium state.

To benchmark the induced plasma environment at different thrust levels, we estimate the average charge exchange ion production rate at thruster exit from these thruster parameters. The average charge exchange ion production rate at thruster exit is given by

$$\frac{dn_{cex0}}{dt} = n_{b0} n_{n0} v_b \sigma_{cex}$$

where $n_{b0} = I_b/ev_bA$ is the average beam ion density at thruster exit, n_{n0} the average neutral density at thruster exit, v_b the beam ion velocity, and σ_{cex} the charge-exchange ion collision cross section.

n_{n0} can be calculated from the measured main flow rate, cathode flow rate, and the discharge propellant efficiency η_d, and by assuming that the un-ionized propellant exits through the grids in free-molecular flow with a temperature close to that of the thruster discharge chamber walls T_w:

$$\dot{n_{n0}} = \frac{\dot{N}}{A_n\sqrt{8kT_w/\pi m_{Xe}}}$$

where $\dot{N}$ is the number of Xe particles per second, and is converted from the discharge charge chamber flow rate, $\dot{m}_d = (1-\eta_d)(\dot{m}_m + \dot{m}_c)$. A_n is the flow-through area through the grids and is about 0.24 of the thruster exit area for the NSTAR thruster. σ_{cex} can be estimated from curve fitting of the measured collision cross section for $Xe^+ - Xe$ charge-exchange [*Rapp*,1962; *Samanata Roy et al.*.1996a]:

$$\sigma_{cex} = (k_1 \ln v_b + k_2)^2 \times 10^{-20}\ m^2$$

where v_b is beam ion velocity with unit in m/s, $k_1 = -0.8821$, and $k_2 = 15.1262$. For the three thrust level considered here, σ_{cex} ranges from 3.65×10^{-15} (cm^2) for ML 6 to 3.37×10^{-15} (cm^2) for ML 83. The calculated beam plasma density, neutral density, and the charge-exchange ion production rate near thruster exit are listed in Table 2. Note that all the parameters listed in Table 2 are averaged estimations at each thrust level because the thruster did not have time to reach its equilibrium condition during S-Peak.

Charge-Exchange Plasma Measured by IDS

Figures 4 and 5 show the data obtained from IDS-RPA and IDS-LP1 during S-Peak, respectively. Figure 4 shows the averaged IDS-RPA sweep curve at each thrust level. Figure 5 shows the averaged IDS-LP1 sweep curve at each thrust level. The voltages measured by the RPA and LP are all relative to the spacecraft ground. From Figure 4, we can obtain the ion current and ion energy relative to the spacecraft potential for each thrust level. From Figure 5, we can obtain the local plasma potential relative to the spacecraft potential. and the electron temperature for each thrust level. Table 3 lists these results.

The observations show that the saturated ion current collected by IDS-RPA increased from $\sim 2.2\ \mu A$ to $\sim 2.4\ \mu A$ when the thrust level changed from ML 6 to ML 36 and decreased to $\sim 1.8\ \mu A$ when the thrust level changed from ML 36 to ML 83. The average energy (relative to spacecraft ground) of the ions collected ranges from 14 eV (at ML 6 and ML 36) to 19 eV (at ML 83). The local plasma potential (relative to spacecraft ground) at IDS location is from 6 Volts (at ML 6) to 4 Volts (at ML 83). The local electron temperature is about 1 to 2 eV.

Since IDS is located well outside of the primary plume region (see Figure 1), the ions collected by IDS-RPA are the charge-exchange ions transported outward from the primary plume. We next derive the charge-exchange ion characteristics from the IDS results. We denote Φ_p, Φ_{IDS}, Φ_{scg} to be the average electrostatic potential inside the thruster plume, the potential at the location of IDS, and the potential of the spacecraft ground, respectively. As the charge-exchange ions originate from the very cold neutrals (temperature 0.04eV), the ion energy measured by RPA represents the difference between the electric potential inside the plume (where these charge-exchange ions are produced) and the spacecraft ground potential, $\Phi_p - \Phi_{scg}$. From the charge-exchange ion energy measured by IDS-RPA and the local plasma potential measured by IDS-LP1, we find the difference between the plume potential and the local plasma potential

$$\Phi_p - \Phi_{IDS} = (\Phi_p - \Phi_{scg}) - (\Phi_{IDS} - \Phi_{scg})$$

Hence, the average energy of the charge exchange Xe^+ ions collected by IDS is $E_{cex} = e(\Phi_p - \Phi_{IDS})$, which gives the average Xe^+ ion velocity at the IDS location

$$v_{cex} = \sqrt{\frac{2e(\Phi_p - \Phi_{IDS})}{m_{Xe}}}$$

From the charge-exchange ion current density measured by RPA, one finds the charge-exchange ion density at the IDS location:

$$n_{cex} = \frac{J_{cex}}{e v_{cex}}$$

The results of the charge-exchange ion plasma environment are listed in Table 4.

We find that the current density associated with charge exchange ion outflow is about $10^{-7} A/cm^2$ and the charge exchange ion density at the IDS location is about $10^6 cm^{-3}$. Not surprisingly, the differences between the charge-exchange ion densities at each thrust level correlates to the changes in the the charge-exchange ion production rate estimated in the previous section. When thrust level changed from ML 6 to ML 36, an increase in the beam ion current drove up d_{cex}/dt, and hence IDS-RPA observed an increase in charge-exchange ion collection. When thrust level changed from ML 36 to ML 83, even though the beam ion current increased, a more significant decrease in the neutral density due to high η_d drove down the d_{cex}/dt, and hence IDS-RPA observed a decrease in charge-exchange ion collection.

The observations show that the plume potential increases significantly as beam current increases. This is not surprising. The propellant plasma plume is a mesothermal plasma, i.e., $v_{ti} << v_b << v_{te}$, where v_{ti}, v_b, and v_{te} are the ion thermal velocity, ion beam velocity, and electron thermal velocity, respectively. When a high density plasma expands into a more dilute plasma under the mesothermal process, the plasma potential decreases as the plasma density decreases. Hence, a larger density difference between the plasma source and the ambient plasma yields a higher potential at the source relative to the ambient. The observations also show that there is an increase in electron temperature as beam current increases. This is probably because that the electrons emitted from the neutralizer undergo a stronger acceleration and heating from the more strong electrostatic field associated with higher plume potential. It is interesting to observe that, while the plume potential $\Phi_p - \Phi_{IDS}$ differs by 60% between the low and high thrust levels, the ratio of the plume potential to the electron temperature is relatively a constant at about $(\Phi_p - \Phi_{IDS})/T_e \sim 7$.

Recently, several computer particle simulation models have been developed for ion thruster charge-exchange plasma[*Samanata Roy*,1996a,b; *Wang et al.*,1996; *Katz et al.*,1997; *Gardner et al.*,1997; *VanGilder et al.*,1997]. In *Wang et al.*[1996], a 3-dimensional electrostatic PIC code coupled with a Monte Carlo collision calculation is used to model the charge-exchange plasma from the DS1 ion thruster. They predicted that, under typical thruster operating conditions, the outflow of charge-exchange Xe^+ should lead to a Xe^+ density of $10^6 cm^{-3}$ and a Xe^+ ion current density of $10^{-7} A/cm^2$ at the IDS location. Similar results were also obtained by *Katz et al.*[1997] and *Gardner et al.*[1997] using a 2-dimensional axis-symmetric finite element particle code. The IDS measurements appear to be in good agreement with these preflight predictions.

4. Summary and Conclusions

For the first time, a comprehensive in-flight investigation of ion propulsion plasma interaction has been carried out on an interplanetary spacecraft, and in situ measurements of the ion propulsion induced plasma environment surrounding an interplanetary spacecraft has been obtained in the solar wind. Analyses of IDS measurements obtained during thruster firings suggest that, at a location about 0.5 meter away from thruster exit, the induced charge-exchange plasma environment has a number density of $\sim 10^6 cm^{-3}$ and an electron temperature of $\sim 1 - 2$eV. The charge-exchange plasma density is about 5 to 6 orders magnitude larger than the solar wind plasma density. The quantitative differences in the measured Xe^+ density at different thrust levels correlates with the charge-exchange ion production rate estimated from thruster data. The potential of the charge-exchange plasma with respect to the IDS location is about $(\Phi_p - \Phi_{IDS})/T_e \sim 7$. However, $(\Phi_p - \Phi_{IDS})$ will increase as the beam current increases. This is because the main underlying physical process that controls the global plume potential is the expansion of the high density propellant plasma. Hence, the plume potential relative to the ambient sensitively depends on the beam ion density. The outflow of charge-exchange Xe^+ ions produces a current density of $\sim 10^{-7} A/cm^2$. These measurements are in good agreement with preflight predictions based on computer particle simulations.

Acknowledgments

We acknowledge technical support provided by the DS1 mission and the NSTAR project. We acknowledge many helpful discussions with D. Young (SwRL), R. Goldstein (SwRL), S.P. Gary (LANL), J. Nordholt (LANL). P.C. Liewer (JPL), B. Goldstein (JPL), and I. Katz (Maxwell Labs). This work was performed by Jet Propulsion Laboratory, California Institute of Technology under a contract with NASA, and was supported by NASA New Millennium Deep Space 1 mission and NASA Solar Electric Propulsion Technology Application Readiness Project.

References

Gardner, B., I. Katz, and V. Davis, Predictions of NSTAR charge-exchange ions and contamination backflow, *IEPC Pap. 97-043*,1997.

Carruth, M., Ed., Experimental and analytical evaluation of ion thruster/spacecraft interactions, *JPL Publication* 80-92, 1981.

Jones, S., J. Staskus, and D. Byers, Preliminary results of SERT II spacecraft potential measurements, *NASA TM X-2083*, 1970.

Katz, I., V. Davis, J. Wang, and D. Brinza, Electrical potentials in the NSTAR charge-exchange plume, *IEPC Pap.* 97-042, 1997.

Kerslake, W., R. Goldman, and W. Nieberding, SERT II: mission, thruster performance, and in-flight thrust measurements, *J. Spacecraft and Rockets*, 8(3), 1971, pp213.

Polk, J., et al., Validation of the NSTAR ion propulsion system on the Deep Space One mission: overview and initial results, *AIAA Pap.* 99-2274, 1999.

Rapp, D. and W. Francis, Charge-exchange between gaseous ions and atoms, *J. Chemical Phys.*, 37(11), 1962, pp2631.

Rayman, M. and D. Lehman, Deep Space One: NASA's first deep-space technology validation mission, *Acta Astronautica*, 41(4), 1997, pp289.

Samanta Roy, R., D. Hastings, and N. Gatsonis, Ion-thruster modeling for backflow contamination, *J. Spacecraft and Rockets*, 33(4), 1996a, pp525.

Samanata Roy, R., D. Hastings, and N. Gatsonis, Numerical study of spacecraft contamination and interactions by ion-thruster effluents, *J. Spacecraft and Rockets*, 33(4), 1996b, pp535.

Wang, J. and J. Brophy, 3D Monte-Carlo particle-in-cell simulations of ion thruster plumes, *AIAA Pap.* 95-2826, 1995.

Wang, J., J. Brophy, and D. Brinza, 3-D simulations of NSTAR ion thruster plasma environment, *AIAA Pap.* 96-3202, 1996.

Worlock, R., E. James, R. Hunter, and R. Bartlett, ATS-6 cesium bombardment engine north-south stationkeeping experiment, *IEEE Trans. Aerospace and Electronic Systems*, ASE-11(6), 1975, pp1176.

VanGilder, D., G. Font, and I. Boyd, Hybrid Monte Carlo particle-in-cell simulation of an ion thruster plume, *IEPC Pap.* 97-182, 1997.

Table 1: S-Peak Thrust Conditions (Jan 22nd, 1999)

Thrust Level	I_b (A)	E_b (eV)	η_d
ML 6	.52	649	.32
ML 36	.82	1003	.52
ML 83	1.40	1095	.88

Table 2: Parameters at Thruster Exit for S-Peak

Thrust Level	J_{b0} (A/m^2)	V_{b0} (km/s)	n_{b0} $(1/cm^3)$	N_{n0} (1/s)	n_{n0} $(1/cm^3)$	dn_{cex0}/dt $(1/cm^3 s)$
ML 6	7.36	29.8	1.54×10^9	6.2×10^{18}	1.4×10^{12}	2.3×10^{13}
ML 36	11.6	37.0	1.96×10^9	4.3×10^{18}	0.95×10^{12}	2.4×10^{13}
ML 83	19.8	38.7	3.22×10^9	1.1×10^{18}	0.23×10^{12}	1.0×10^{13}

Table 3: IDS Results

Thrust Level	I (μA)	E_{cex} (eV)	T_e (eV)	$\Phi_{IDS} - \Phi_{scg}$ (V)
ML 6	2.2	15	1.17	6
ML 36	2.4	14	1.33	5
ML 83	1.8	19	2.09	4

Table 4: Induced Plasma Environment at IDS

Thrust Level	$\Phi_p - \Phi_{IDS}$ (V)	$(\Phi_p - \Phi_{IDS})/T_e$	J_{cex} (A/cm^2)	v_{cex} (km/s)	n_{cex} (cm^{-3})
ML 6	9	7.7	1.1×10^{-7}	3.45	2×10^6
ML 36	9	6.8	1.2×10^{-7}	3.45	2.2×10^6
ML 83	15	7.2	0.9×10^{-7}	4.46	1.2×10^6

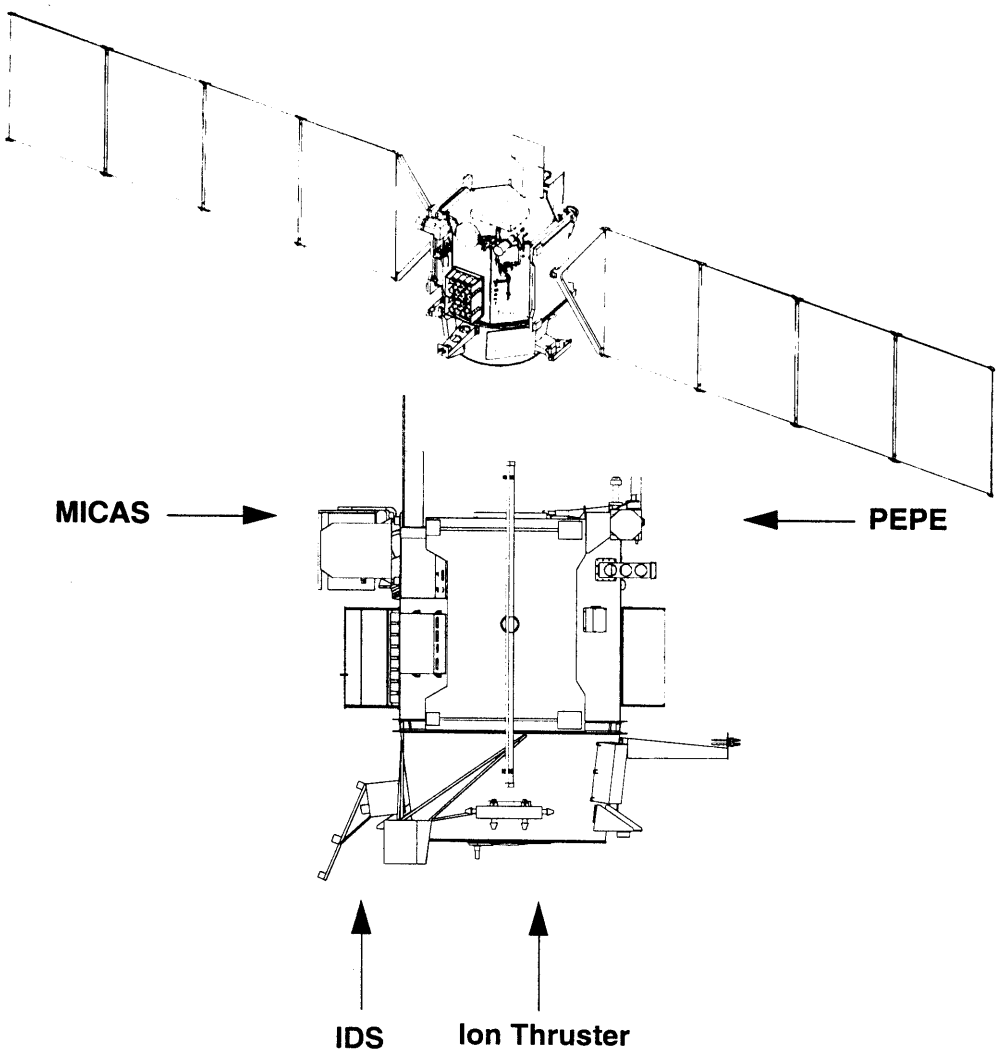

Figure 1 Illustration of the Deep Space 1 Spacecraft

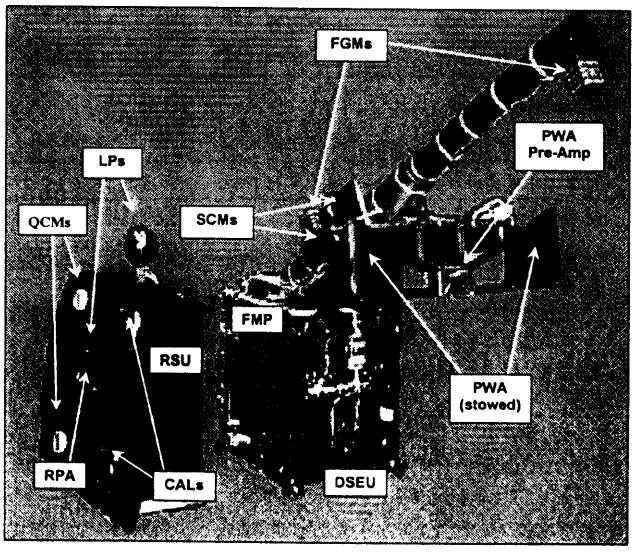

Figure 2: The Ion Propulsion Diagnostic Subsystem

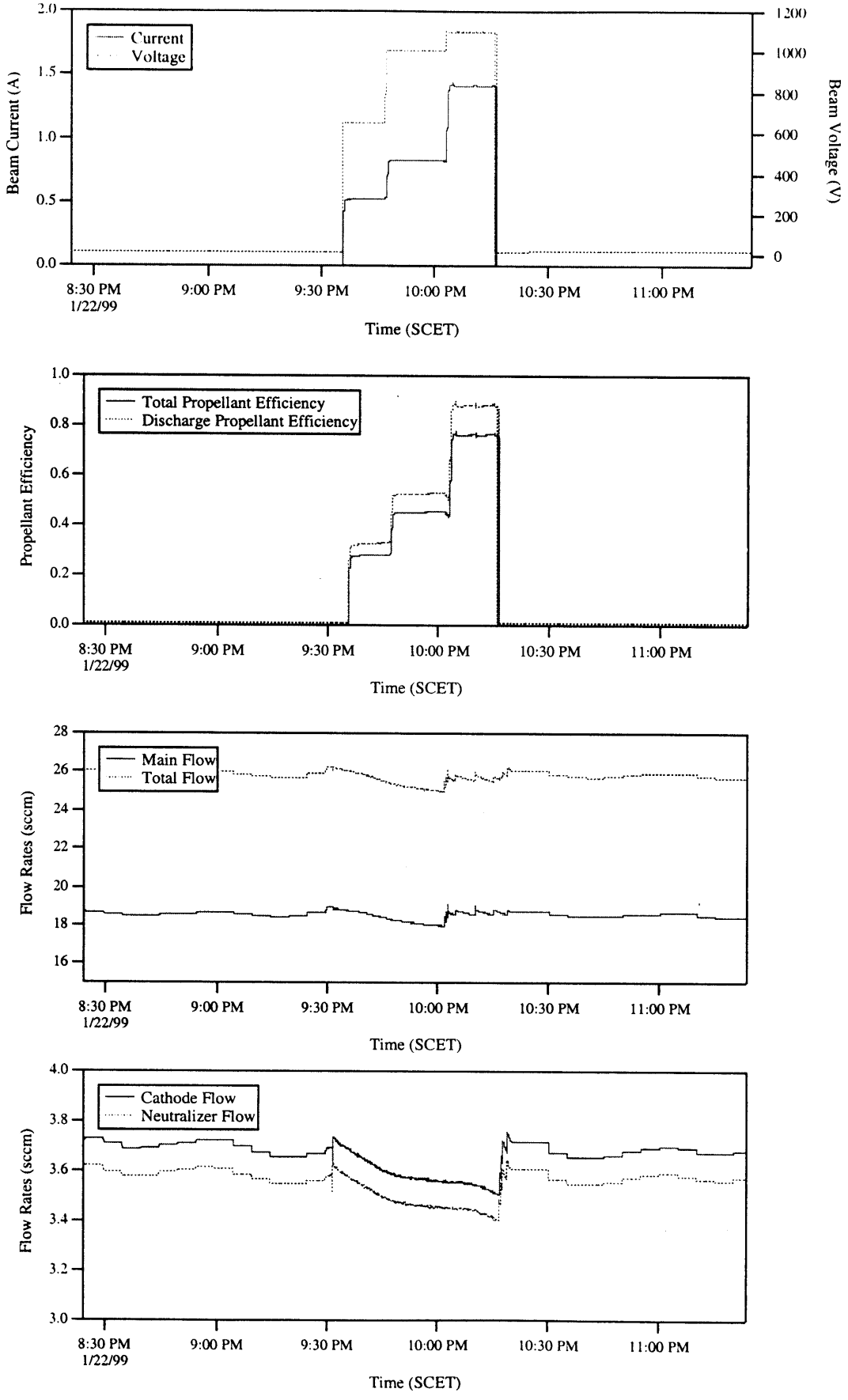

Figure 3 Thruster Parameters obtained from DS1 flight data for S-Peak

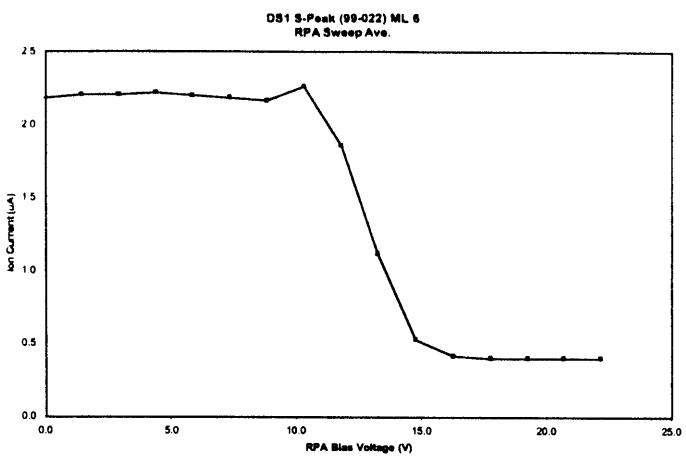

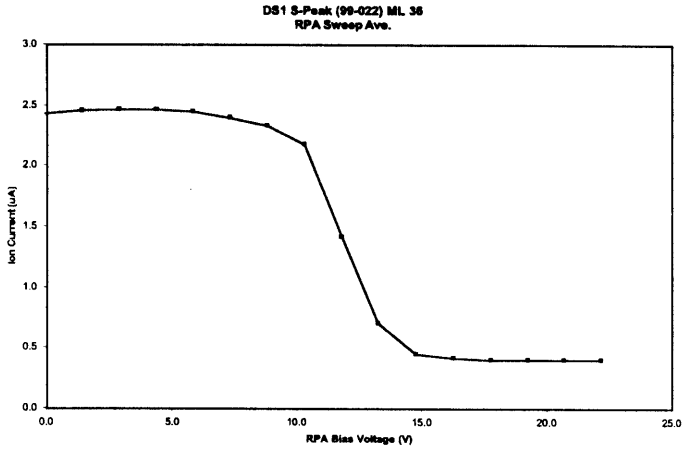

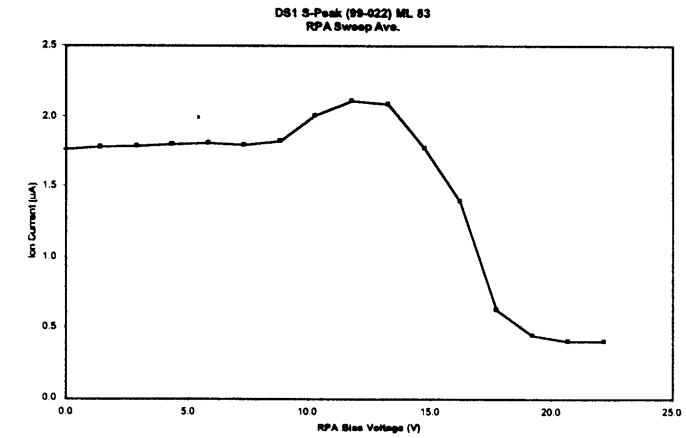

Figure 4 IDS-RPA sweep curve averaged for each thrust level

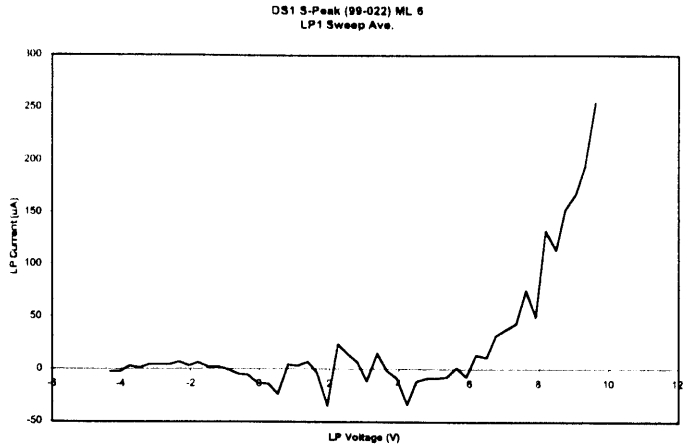

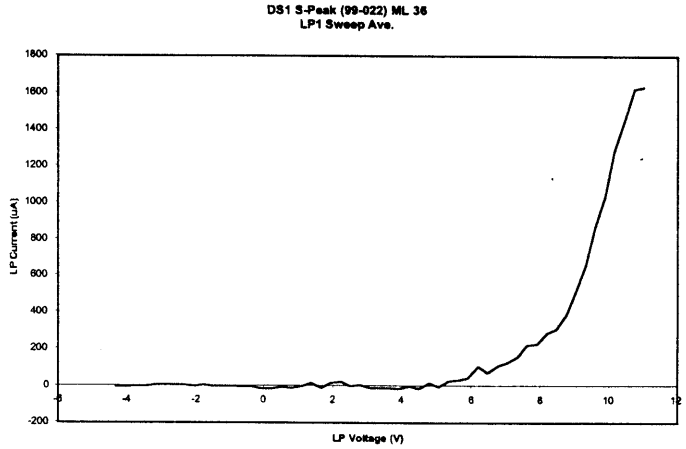

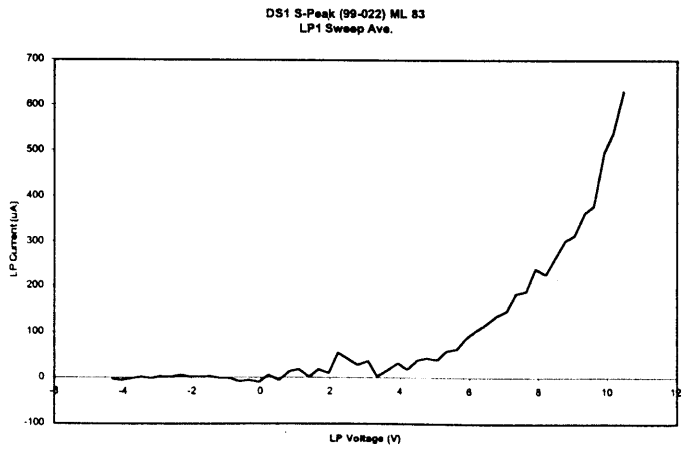

Figure 5 IDS-LP1 sweep curve averaged for each thrust level